Author(s): Rigaud, Cyril; Eriksson, Andreas; Krasnov, Aleksei; Wincent, Emma; Pakkanen, Hannu; Lehtivuori, Heli; Ihalainen, Janne; Vehniäinen, Eeva-Riikka

Title: Retene, pyrene and phenanthrene cause distinct molecular-level changes in the cardiac tissue of rainbow trout (Oncorhynchus mykiss) larvae, part 1 – Transcriptomics

Year: 2020

Version: Accepted version (Final draft)

Please cite the original version:

Rigaud, C., Eriksson, A., Krasnov, A., Wincent, E., Pakkanen, H., Lehtivuori, H., Ihalainen, J., & Vehniäinen, E.-R. (2020). Retene, pyrene and phenanthrene cause distinct molecular-level changes in the cardiac tissue of rainbow trout (Oncorhynchus mykiss) larvae, part 1 – Transcriptomics. Science of the Total Environment, 745, 141031. https://doi.org/10.1016/j.scitotenv.2020.141031

Retene, pyrene and phenanthrene cause distinct molecular-level changes in the cardiac tissue of rainbow trout (Oncorhynchus mykiss) larvae, part 1 – Transcriptomics

Cyril Rigaud, Andreas Eriksson, Aleksei Krasnov, Emma Wincent, Hannu Pakkanen, Heli Lehtivuori, Janne Ihalainen, Eeva-Riikka Vehniäinen

PII: S0048-9697(20)34560-5

DOI: https://doi.org/10.1016/j.scitotenv.2020.141031

Reference: STOTEN 141031

To appear in: *Science of the Total Environment*

Received date: 7 May 2020

Revised date: 29 June 2020

Accepted date: 15 July 2020

Please cite this article as: C. Rigaud, A. Eriksson, A. Krasnov, et al., Retene, pyrene and phenanthrene cause distinct molecular-level changes in the cardiac tissue of rainbow trout (Oncorhynchus mykiss) larvae, part 1 – Transcriptomics, *Science of the Total Environment* (2020), https://doi.org/10.1016/j.scitotenv.2020.141031

Title

Retene, pyrene and phenanthrene cause distinct molecular-level changes in the cardiac tissue of rainbow trout (*Oncorhynchus mykiss*) larvae, Part 1 – Transcriptomics

Authors

Cyril Rigaud [a,*], Andreas Eriksson [a], Aleksei Krasnov [b], Emma Wincent [c], Hannu Pakkanen [a], Heli Lehtivuori [d], Janne Ihalainen [a] and Eeva-Riikka Vehniäinen [a]

Affiliations

[a] Department of Biological and Environmental Sciences, University of Jyväskylä, Jyväskylä, Finland

[b] Norwegian Institute of Food, Fisheries and Aquaculture Research, Ås, Norway

[c] Institute of Environmental Medicine, Karolinska Institutet, Stockholm, Sweden

[d] Department of Physics, Nanoscience Center, University of Jyväskylä, Jyväskylä, Finland

* Address correspondence to cyril.c.rigaud@jyu.fi

Abstract

Polycyclic aromatic hydrocarbons (PAHs) are contaminants of concern that impact every sphere of the environment. Despite several decades of research, their mechanisms of toxicity are still poorly understood. This study explores the mechanisms of cardiotoxicity of the three widespread model PAHs retene, pyrene and phenanthrene in the rainbow trout (*Oncorhyncus mykiss*) early life stages. Newly hatched larvae were exposed to each individual compound at sublethal doses causing no significant increase in the prevalence of deformities. Changes in the cardiac

transcriptome were assessed after 1, 3, 7 and 14 days of exposure using custom *Salmo salar* microarrays. The highest number of differentially expressed genes were observed after 1 or 3 days of exposure, and retene was the most potent compound in that regard. Over-representation analyses suggested that genes related to cardiac ion channels, calcium homeostasis and muscle contraction (actin binding, troponin and myosin complexes) were especially targeted by retene. Pyrene was also able to alter similar myosin-related genes, but at a different timing and in an opposite direction, suggesting compound-specific mechanisms of toxicity. Pyrene and to a lesser extent phenanthrene were altering key genes linked to the respiratory electron transport chain and to oxygen and iron metabolism. Overall, phenanthrene was not very potent in inducing changes in the cardiac transcriptome despite being apparently metabolized at a slower rate than retene and pyrene. The present study shows that exposure to different PAHs during the first few days of the swim-up stage can alter the expression of key genes involved into the cardiac development and function, which could potentially affect negatively the fitness of the larvae in the long term.

Keywords: aquatic toxicology**,** cardiotoxicity, polycyclic aromatic hydrocarbons (PAHs), transcriptomics

1. Introduction

Polycyclic aromatic hydrocarbons (PAHs) are widespread contaminants coming from both pyrogenic or petrogenic sources, which can be from natural or anthropogenic origins. Due to atmospheric deposition, municipal and industrial effluents, surface runoffs, natural and accidental oil seeps or spills, the aqueous environment is quite often the ultimate recipient for most PAHs (Wolska et al., 2012). Because of increasing anthropogenic activities, the influx of PAHs to the aquatic environment is believed to have increased over the past decades (Kurek et

al., 2013). Consequently, aquatic organisms are chronically exposed to PAHs directly via the water column, by contact with the sediment or by ingesting contaminated prey (Logan, 2007).

PAHs are known to be very potent embryotoxic compounds to fish and induce various negative effects such as oxidative stress, DNA damage, disruption of the thyroid and endocrine function (He et al., 2012; Le Bihanic et al., 2014; Madison et al., 2015). Some PAHs are able to interact with the aryl hydrocarbon receptor (AhR) and produce dioxin-like toxicity (Billiard et al., 1999; Incardona et al., 2006; Scott et al., 2011). Dioxin-like toxicity in fish is characterized by the blue sac disease (BSD) syndrome, which includes various symptoms such as the induction of cytochrome P4501A (CYP1A) detoxification enzymes, developmental arrest, craniofacial deformities, cardiovascular defects, pericardial and yolk sac edemas, hemorrhages and eventually death. The heart is a primary target of dioxin-like compounds, and defects in the cardiovascular tissue are among the first observable symptoms of dioxin-like embryotoxicity in fish (Doering et al., 2019). The AhR is a transcription factor, which after activation by agonists such as dioxin-like compounds (DLCs) or PAHs translocates to the nucleus and alters the transcription of numerous genes linked for example to signal transduction, cell growth and proliferation, cardiovascular development and the cell cycle (Larigot et al., 2018). Unlike most legacy DLCs (such as dioxins, furans or coplanar polychlorinated biphenyls) for which the binding affinity for the AhR is assumed as the main factor predicting their embryotoxic potency, other factors need to be considered in the case of PAHs. While most legacy DLCs are known to be very persistent, PAHs are readily metabolized by fish, and differences in their metabolism among compounds and species seem to play a role regarding their embryotoxic potency (Billiard et al., 2008; Jung et al., 2015). PAH embryotoxicity varies with interactions among rates of uptake, metabolism and excretion (Hodson, 2017). Slow diffusion across the chorion can for

example lower their embryotoxic potential (Brinkworth et al., 2003). The persistence of PAHs in fish depends on their potency for CYP1A induction, which is a function of their binding affinities to the AhR, and CYP1A induction can both increase and decrease their embryotoxicity (Hodson, 2017). Oxygenation of PAHs can produce toxic metabolites such as phenols, benzylic alcohols, epoxides, quinones and reactive intermediates (Tabash, 2003). However, though their toxicity has been studied for more than 20 years, the mechanisms of toxicity of PAHs following activation of the AhR are still not well characterized.

Among PAHs, retene (7-isopropyl-1-methylphenantrene) is an alkylated three-ring PAH originating from forest fires or pulp and paper mill effluents (Leppänen and Oikari, 2001; Shen et al., 2012) that has been shown to be a potent AhR agonist capable of inducing BSD symptoms in different fish species (Billiard et al., 1999; Scott et al., 2011). Retene has recently been reported at concentrations in the $ng.L^{-1}$ range in the surface water and in the $ng.g^{-1}$ range in the sediment of North American lakes (Ahad et al., 2015; Ruge et al., 2015). In areas contaminated by pulp and paper mill effluents, concentrations up to several hundreds or thousands of $\mu g.g^{-1}$ in the sediment have been reported (Leppänen and Oikari, 2001; Meriläinen et al., 2006). Vehniäinen et al. (2016) found that a sublethal dose of retene was able to induce significant changes in the cardiac transcriptome of rainbow trout (*Oncorhynchus mykiss*) larvae, potentially disturbing several key processes related to cardiovascular development and function. More recently, retene was shown to alter the action potential as well as the intensity of key cardiac ionic currents (calcium, potassium and sodium) *in vitro* in rainbow trout ventricular cardiomyocytes (Vehniäinen et al., 2019).

Pyrene is a ubiquitous four-ring PAH, found to be among the dominant PAH compounds in the air, in precipitation water and in coastal and estuarine waters and sediments (Latimer and Zheng,

2003). Pyrene concentration in surface water can reach concentrations in the $\mu g.L^{-1}$ range in heavy industrial areas, and even up to several hundreds of $\mu g.L^{-1}$ in marine samples close to crude oil exploitation areas (Anyakora et al., 2005; Maskaoui et al., 2002). Like retene, it is also capable of binding with the AhR and of producing dioxin-like toxicity in various fish species (Hendon et al., 2008; Incardona et al., 2006; Shi et al., 2012; Zhang et al., 2012). However, it is known to be a much weaker AhR agonist than retene (Barron et al., 2004). While the knockdown of *cyp1a* (the cytochrome P4501A gene) by morpholino oligonucleotides does not appear to affect retene toxicity in zebrafish (*Danio rerio*) embryos (Scott et al., 2011), it delayed noticeably the onset of toxicity of pyrene in the same species (Incardona et al., 2005). This suggests different toxicodynamics and molecular targets between retene and pyrene downstream of AhR activation. A low-level pyrene exposure causing no significant increase in the expression of *cyp1a* was able to significantly alter the cardiac function (increased heart rate) of 72 HPF (hours post-fertilization) zebrafish larvae, suggesting AhR-independent cardiotoxicity (Zhang et al., 2012).

Phenanthrene is a three-ring PAH that is, like pyrene, found among the most abundant PAH compounds in the environment (Latimer and Zheng, 2003). Similar to pyrene, phenanthrene was reported at concentrations in the $\mu g.L^{-1}$ range in surface waters impacted by industrial areas, and up to several hundreds of $\mu g.L^{-1}$ in areas affected by crude oil exploitation (Anyakora et al., 2005; Maskaoui et al., 2002). Unlike retene and pyrene, phenanthrene is a very weak AhR agonist (Bak et al., 2019; Barron et al., 2004). However, phenanthrene is still able to negatively impact the cardiac morphology of the heart in fish embryos by producing abnormal heart looping, pericardial edemas, as well as affecting the cardiac function by causing significant changes in the cardiac rhythm, blockage of the atrioventricular conduction or reduction of blood

circulation (Cypher et al., 2017; Incardona et al., 2004; Mu et al., 2014; Sun et al., 2015; Zhang, Huang, Wang et al., 2013; Zhang, Huang, Zuo et al., 2013). The ability of phenanthrene to alter the cardiac function in fish may be partially explained by its potency to modulate the ion currents and action potential, as demonstrated *in vitro* in cardiomyocytes of several fish species (Ainerua et al., 2020; Brette et al., 2017; Vehniäinen et al., 2019), including the rainbow trout.

The aim of the present study was to explore and compare the molecular mechanisms of cardiotoxicity of three model PAHs, i.e. retene, pyrene and phenanthrene, in rainbow trout early life stages (ELS). The hypothesis of the present study was that the tested PAHs will cause specific effects on the cardiac transcriptome of the rainbow trout larvae, and that these changes could point to potential mechanisms of toxicity. Larvae were exposed immediately after hatch in a semi-static setup to sublethal doses of each individual PAH. Changes in the cardiac transcriptome were assessed by microarray after 1, 3, 7 or 14 days of continuous exposure. Microarray analyses measure the expression of numerous genes in parallel. By combining both hypotheses-driven and hypotheses-free research strategies, they allow exploring for potential molecular mechanisms and novel biomarkers (Krasnov et al., 2011). The present manuscript is part of a larger project in which several OMICs tools were combined in an attempt to better understand the mechanisms of toxicity of those compounds: the changes in the cardiac proteome and metabolome following exposure to those model PAHs were also assessed using a similar experimental setup.

2. Materials and methods

2.1. Chemicals

Retene (≥98% purity) was purchased from MP Biomedicals (Illkirch, France). Pyrene (>98% purity), phenanthrene (≥99.5% purity) and dimethyl sulfoxide (DMSO, anhydrous, ≥99.9% purity) were obtained from Sigma-Aldrich (St-Louis, MO, USA). Stock solutions of each individual PAH were prepared by dissolving them in DMSO to reach concentrations of 3.2 $mg.mL^{-1}$ for retene and pyrene, and 10 $mg.mL^{-1}$ for phenanthrene.

2.2. Experimental design

For each experiment, exposure tanks (N = 52) were prepared one day before the start of the exposures and consisted of 1.5L Pyrex glass bowls filled with 1L of filtered lake water (Lake Konnevesi, Konnevesi, Finland). The dissolved organic carbon (DOC) in the filtered lake water ranged between 7,0 and 8,2 $mg.L^{-1}$ (unpublished results). Tanks were randomly separated between four different treatments (N = 13 tanks per treatment): DMSO (0.001%), retene (RET, 32 $\mu g.L^{-1}$), pyrene (PYR, 32 $\mu g.L^{-1}$) and phenanthrene (PHE, 100 $\mu g.L^{-1}$). The amount of DMSO per tank was the same in all tanks (10 µL of pure DMSO or of the appropriate PAH stock solution into 1L of lake water). These exposure concentrations were selected based on previous studies in the case of retene (Billiard et al., 1999), and from preliminary experiments (unpublished results) in the case of pyrene and phenanthrene. The concentrations retained were sublethal but still able to cause cardiotoxic effects such as pericardial edemas and arrhythmias. Rainbow trout eyed embryos at 360 degree-days (°D) of development were obtained from a local fish farm (Hanka-Taimen, Hankasalmi, Finland). Though the larvae used in this study are defined as eleuthero embryos and therefore no animal permit was required, fish handling and sampling were performed in a way that minimizes animal suffering as well as the number of individuals required. Newly hatched embryos without apparent deformities (i.e. presenting no visible edemas, hemorrhages or abnormal curvature of the tail) were then randomly distributed

into twelve exposure tanks per treatment (N = 15 embryos per tank, 720 embryos in total), leaving four tanks (one per treatment) without fish for PAH concentration measurements purpose. Embryos were monitored daily for mortality, and the exposure water was completely renewed daily as well: fresh chemicals were added to ensure constant exposure to PAHs (semi-static exposure). Water temperature was measured every day and parameters such as pH, conductivity and dissolved oxygen were monitored on a regular basis. The light:dark cycle was set on 16h:8h, and yellow fluorescent tubes were used.

The procedure described above was repeated three different times, for three different experiments, each corresponding to a different exposure time: larvae were sampled after either 1, 3 or 7 days of exposure. These time points were selected to assess the effects of a short-term exposure on the cardiac transcriptome, before the first signs of cardiotoxicity that are typically observed after 3 to 7 days. A fourth experiment, which consisted of 14 days of exposure, was also performed with slightly different N parameters: only 9 tanks per treatment were used, including one without fish. This exposure was performed to assess for potential long-lasting effects of the tested PAHs on the cardiac transcriptome. At sampling day, three random larvae per tank (N = 36 per treatment, 24 for the 14 days exposure) were photographed for morphometric analyses: larvae length and yolk sac area were measured later using the ImageJ software (Rueden et al., 2017). All larvae were monitored for signs of BSD (pericardial and yolk sac edemas, hemorrhages, craniofacial and spinal deformities) and a severity index ranging from 0 to 1 was calculated for each tank according to the scoring scheme of Villalobos et al. (2000) with the modifications from Scott and Hodson (2008). Larvae were then quickly and carefully dissected under the microscope: the heart of each larva was separated from the rest of the body using fine forceps (Dumont #5, Fine Science Tools, Heidelberg, Germany). The hearts of the

larvae from three different tanks per treatment were pooled together (only two tanks for the 14 days exposure), thus each treatment consisted of four samples containing 45 hearts each (30 hearts for the 14 days exposure). A total of 64 samples (N = 4 for each of the four treatments and each of the four time points) were kept in liquid nitrogen during sampling and stored at -80°C until further analyses.

2.3. Measurements of PAHs concentration in water

Depending on the duration of the experiment, water samples were collected after 1, 3, 7, 10 and 14 days of exposure, before the daily exposure water renewal. Previous studies showed that concentrations measured by SFS right after the daily renewal are close to the nominal values (Honkanen et al., 2020; unpublished results). Collection was performed by pipetting 5 mL of exposure water from four tanks per treatment, as well as from each tank set without fish at the beginning of the experiment (one per treatment). After the addition of 5 mL of ethanol (99.5% purity), samples were stored in 20 mL scintillation vials at 4°C until further analyses.

Synchronous fluorescence spectroscopy (SFS) measurements were performed using a LS-55 Fluorescence Spectrometer (PerkinElmer, Waltham, MA, USA). Readings were performed in quartz cuvettes for retene and phenanthrene (Quartz SUPRASIL® High Precision Cell, Hellma Analytics, Müllheim, Germany) and in disposable plastic cuvettes (BRAND GMBH, Wertheim, Germany) for pyrene. Quartz was favorized over plastic for retene and phenanthrene because of the very low fluorescence observed for these compounds at the tested concentrations. The fluorescence values were so high with pyrene that the absorbance spectra of the plastic cuvettes were not a problem when performing the measurements.

SFS parameters were obtained from Turcotte et al. (2011) and Watson et al. (2004), with some minor modifications. Some parameters were fixed for all compounds: the scanning speed was 150 $nm.min^{-1}$, and both excitation and emission slits were 5 nm for all measurements. The scanning ranges for retene, pyrene and phenanthrene were set on 290-350, 300-400 and 270-320 nm, respectively. The delta wavelengths ($\Delta\lambda$) for retene, pyrene and phenanthrene were set on 50, 37 and 56 nm, respectively. Standard curves were prepared for each compound, and the peak areas of retene (290-315 nm) and phenanthrene (284-302 nm) were used to estimate their respective concentrations in the samples, after normalization against their respective controls. This method was not possible with pyrene since its metabolites were also showing up in the fluorescence spectrum and partially overlapping with its fluorescence peak (329-342 nm). Instead, the maximum peak height of pyrene was used to estimate pyrene concentration in the samples. This maximum value was localized using the standards and was measured at 333.5 or 334 nm. Standard curves for pyrene were calculated accordingly, and the data for pyrene samples was normalized against their respective controls as well.

2.4. Measurement of total PAH content in larvae

PAHs were extracted and measured from 12 random larvae per tank (without the heart tissues used for RNA extraction), and from 8 tanks per treatment (N = 8). Larvae from a single tank were pooled and homogenized into 600 µL of 70% acetonitrile (ACN, Thermo Fisher Scientific, Waltham, MA, USA) with a bullet blender (Next Advance, Troy, NY, USA) set on the maximum settings, following the addition of eight 1 mm and four 2 mm ∅ zirconium IV oxide pellets (Next Advance). The homogenate was then centrifuged for 15 minutes at 14000 rpm and 4°C (Centrifuge 5415R, Eppendorf, Hamburg, Germany). The supernatant was collected and the

remaining pellet was resuspended and centrifuged three more times in 400 µL of 70% ACN. The total volume of supernatant was pooled and stored at -20°C until further analyses.

A subsample of the supernatant was analyzed with a Shimadzu HPLC system (SIL-30AD coupled to a SIL-30AC, SPD-M20A and CT20AC) (Shimadzu, Kyoto, Japan) coupled to a 150 mm long ACE C18-AR column with a particular size exclusion of 5 µm (Advanced Chromatography Technologies Ltd, Aberdeen, Scotland) and a RF-20Axs Prominence fluorescence detector (Shimadzu). The developed protocol allowed us to detect any of the three target PAHs (retene, pyrene and phenanthrene) in one single run. For retene, pyrene and phenanthrene respectively, excitation was set at 259, 335 and 252 nm; emission was set at 370, 383 and 364 nm; retention time was equal to 16.71 ± 0.09, 14.18 ± 0.12 and 12.00 ± 0.02 minutes. The analytic protocol was run at 1.0 $mL.min^{-1}$ over a ddH2O + 1.5 mM formic acid (Thermo Fisher Scientific) coupled to a 70% ACN + 1.5 mM formic acid gradient ranging from a 50:50 ratio at the start to 100% ACN + formic acid after 15 minutes and then back to 50:50 between minutes 16 and 20. Standard curves were generated by diluting 0.005, 0.022 and 0.086 nM of retene; 0.006, 0.025 and 0.098 nM of pyrene; and 0.0005, 0.0056 and 0.056 nM of phenanthrene in 70% ACN. Concentrations were calculated according to the standard curves, corrected for background noise (DMSO control samples) and finally expressed as the average PAH load per larva (ng of PAH per larva).

2.5. Microarray analysis

Total RNA was extracted from the heart samples using TRI Reagent (Molecular Research Center, Cincinnati, OH, USA) following the manufacturer's instructions. A NanoDrop™ (Thermo Fisher Scientific, Waltham, MA, USA) device was used to measure RNA quantity, as well as its purity using the 260-280 nm optical density ratio. The quality of the RNA was then

measured with an Agilent 2100 Bioanalyzer (Agilent Technologies, Santa Clara, CA, USA) following the manufacturer's instructions; the lowest RIN (RNA Integrity Number) measured in this study was equal to 9.8. For each sample, half of the RNA was saved for microarray analyses, and the other half was saved for the qPCR (quantitative real-time PCR) validation of the microarray results. The qPCR validation methods and results can be found in the Supplementary file 1.

Of the 64 RNA samples, 48 were used for the microarray analyses: 3 per treatment and time point. A total input amount of 220 ng of RNA per sample was amplified and labeled with the Cy3 dye using the one-color Agilent Low Input Quick Amp Labeling Kit (product number 5190-2305). The amplified/labeled cRNA was then purified with the Qiagen RNeasy Mini Kit (Qiagen, Hilden, Germany). A NanoDrop™ device was used to measure the concentration of Cy3 and cRNA, allowing us to calculate the specific activity (pmol of Cy3 per µg of cRNA) of each sample. The average cRNA concentration in the samples was equal to 266.3 ± 48.9 ng.µL^{-1}, and the average specific activity was equal to 12.9 ± 3.6 pmol of Cy3 per µg of cRNA. A total of 3 samples were below the recommended specific activity of 8.0 pmol of Cy3 per µg of cRNA but were included in the rest of the analyses nonetheless. A subsample equivalent to 1650 ng of Cy3-labeled cRNA was hybridized to Agilent 4x44k custom arrays (*Salmo salar* Salgeno-1 array, design ID 082522) using the Agilent Gene Expression Hybridization Kit (product number 5188-5242) and incubated overnight at 65°C. Details about the selection and annotation of the mRNAs sequences as well as the design of the 4x44k custom array used in the present study can be found in Krasnov et al. (2011). Hybridization washes were performed the following day using the Agilent Gene Expression Wash Buffer Kit (product number 5188-5327). Array readings were performed using an Agilent SureScan Microarray Scanner. The gene expression data was

processed and analyzed with the help of the bioinformatics package described in Krasnov et al. (2011). The mean intensities of all arrays were normalized and the individual values of each feature were divided by the mean values of all samples. Significantly differentially expressed genes (DEGs) were determined by difference from their respective controls (Student's *t*-test, $p \leq 0.05$). The data was expressed as $\log_2$ of the fold changes ($\log_2$-FC) compared to the respective control. The list of all DEGs is available in the Supplementary file 2.

In order to explore the possible mechanisms of toxicity involved with the PAHs used in the present study, over-representation analyses (ORAs) were performed. ORA (Boyle et al., 2004) is a widely used approach to determine whether known biological functions or processes are over-represented in an experimentally-derived gene list (Yu et al., 2012). ORAs were done using R 3.5.1 (The R Foundation for Statistical Computing), Bioconductor 3.7 and the over-representation test feature implemented in the R package clusterProfiler 3.8.1 (Yu et al., 2012). Because the test requires the use of an organism database that is available in the AnnotationHub web resource, a zebrafish (*Danio rerio*) RefSeq gene ID and gene symbol was attributed to each feature of the array used in the present study. This was achieved using the NCBI BLAST software 2.7.1 (National Center for Biotechnology Information, Bethesda, MD, USA): the whole NCBI nucleotide database was used to generate a custom-made sub-database containing all sequences associated with the zebrafish taxonomic ID (i.e. 7955). The GenBank nucleotide accession numbers of the features from the array used in the present study were used to extract the corresponding FASTA coding sequences with the NCBI Batch Entrez online tool. Those FASTA sequences were then blasted against the custom-made zebrafish database mentioned above. The BLAST output was filtered to remove matches with *E*-values $\geq 10^{-3}$. A list of 19025 unique zebrafish gene IDs was obtained and used as a background for the ORAs. Only the

significant DEGs for which a zebrafish ID could be attributed were included in the ORAs. ORAs were performed for each of the three categories of the Gene Ontology (GO) annotations database: biological process (BP), molecular function (MF) and cellular component (CC) (Ashburner et al., 2000). ORAs were also performed for the KEGG (Kyoto Encyclopedia of Genes and Genomes, Kyoto University, Japan) pathways and Reactome pathways databases. *P*-values were adjusted (*p*-adjust) for multiple comparisons using the Benjamini and Hochberg (BH) method, which control the false discovery rate (FDR), i.e. the expected proportion of false discoveries among the rejected hypotheses (Benjamini and Hochberg, 1995). The significant threshold for the adjusted *p*-values was set at $\alpha = 0.05$.

2.6. Statistical analyses

Statistical analyses were performed using R 3.5.1 (The R Foundation for Statistical Computing) with the significant level set at $\alpha = 0.05$. When the data was expressed as proportions (%) of individuals, for example for mortality, differences among treatments were assessed using the Fisher's exact test (FE). Morphometric data (body length and yolk sac area) was adjusted according to effective degree-days (Kamler, 2002) and normalized against one of the control tanks: this normalization was performed to account for possible water temperature differences among tanks or experiments. The normal distribution of the data was assessed with the Shapiro-Wilk test. Differences among treatments were assessed using a one-way ANOVA for normally distributed data and a non-parametric Kruskal-Wallis test (KW) otherwise. If significant differences were detected, it was followed by a multiple comparisons Tukey's HSD test in the case of an ANOVA or a Conover's test in the case of a KW. The microarray data statistical analyses were detailed above.

3. Results

3.1. Mortality and morphometry

None of the tested PAHs concentrations significantly increased the mortality of the larvae at any time point, compared to the control groups (FE, $p > 0.05$, data not shown). The highest mortality observed was equal to 5.08% (2.35-10.64) and occurred in the larvae group exposed to pyrene for 14 days (% mortality and 95% confidence interval). The mortality of the control groups ranged from 0% (0-2.09) to 3.36% (1.31-8.32) across all experiments. The complete mortality data can be found in the Supplementary file 1. None of the PAHs caused significant effects on body length or yolk sac area at any time point (ANOVA or KW, $p > 0.05$, data not shown). The BSD severity index of the control groups ranged from 0.03 ± 0.02 to 0.27 ± 0.06 across all experiments (mean ± SD). The BSD severity index was significantly increased following exposure to retene (0.38 ± 0.07) and phenanthrene (0.36 ± 0.07) after 3 days of exposure (KW, $p = 0.009$, data not shown), but not by pyrene or at other time points.

3.2. Water parameters and PAHs concentrations

The characteristics of the filtered lake water used in the present study were the following: conductivity 24.7 ± 1.1 µS, pH 7.27 ± 0.09 and oxygen saturation > 94%. The average temperatures were equal to 11.6 ± 0.3, 11.4 ± 0.4, 11.7 ± 0.3 and 11.6 ± 0.4°C for 1, 3, 7 and 14 days exposure, respectively. Retene, pyrene and phenanthrene were undetected in control tanks at any time point. The average concentration over time of retene and pyrene in tanks without larvae were equal to 10.66 ± 3.92 and 8.84 ± 1.99 $\mu g.L^{-1}$, thus roughly equivalent to one third and one quarter of the nominal concentration (32 $\mu g.L^{-1}$) for those compounds. The average concentration over time of phenanthrene in the tanks without larvae was equal to 5.82 ± 3.74 $\mu g.L^{-1}$, almost 20 times lower than the nominal concentration. In the presence of larvae, the concentrations of retene and pyrene measured in the water tended to decrease over time, while no

particular trend was observed for phenanthrene (Fig. 1A). Due to the detection of pyrene metabolites in the fluorescence spectrums for pyrene water samples (Fig. 1B), pyrene concentrations could not be calculated using the same method as for retene and phenanthrene water samples (see subsection 2.3.). No metabolites were detected in the tanks without larvae, while at least one metabolite peak was detected (around 342 nm) already after 1 day of exposure in the presence of larvae. This peak increased until 7 days of exposure and then decreased at 10 and 14 days. Another peak located around 360 nm could be observed after 7 and 14 days of exposure, and to a lower extent after 3 and 10 days as well.

The total content of each PAH was also measured in the larvae remaining bodies (without the heart tissues) by HPLC at the end of each exposure (1, 3, 7 or 14 days) (Fig. 2). Differences of at least one order of magnitude were observed between compounds, with retene being the PAH measured at the lowest values (less than 1 ng per larva) and phenanthrene at the largest (several hundreds of ng per larva). The total content of retene measured in the larvae tended to decrease over time, while no particular trend was observed for pyrene and phenanthrene (Fig. 2).

3.3. Microarray analysis output

The effects of retene, pyrene and phenanthrene on the cardiac transcriptome of rainbow trout larvae were investigated by microarray analysis. The qPCR results were in most cases well in line with the microarray results (Supplementary file 1). Retene was the most potent compound in terms of observed DEGs, with the highest number of genes affected after 1 and 3 days of exposure (Fig. 3). Very few DEGs were shared between compounds, with the exception of pyrene and phenanthrene after 1 day of exposure where 18 DEGs were found to be downregulated by both compounds (Fig. 3). The list of all DEGs is available in the Supplementary file 2.

An overview of the ORAs is shown in figure 4. For each treatment and time point presented in figure 4, a more detailed view of all over-represented GO terms and the genes involved in each of them (as well as their fold changes) is available in figures 5 and 6. The over-represented GO terms found for retene after one day of exposure were mostly associated with cation transport (Fig. 4. and 5). The GO terms over-represented after 3 days of exposure to retene appeared to be mostly linked to the cytoskeleton and muscle fibers (actin binding, troponin complex, myosin complex, etc.) (Fig. 4 and 5). The GO term myosin complex that was found after 3 days of exposure to retene was also found after 1 day of exposure to pyrene (Fig. 4). While those myosin-related genes were mostly downregulated by retene, pyrene caused the opposite effect with most genes being upregulated (Fig. 5 and 6). No GO terms were found to be over-represented after 3 or 7 days of exposure to pyrene, while most of the GO terms over-represented after 14 days were related to xenobiotic metabolism, the respiratory electron chain, iron metabolism and the hemoglobin complex (Fig. 6). Genes related to the hemoglobin complex and iron metabolism were also over-represented in the case of 14 days of exposure to phenanthrene (Fig. 6). The gene named *zgc:173594* (Fig. 6) is assumed to be involved in cellular iron ion homeostasis and iron ion transport (according to the ZFIN database) and was linked to ferritin in the microarray *S. salar* features (Supplementary file 2). Another gene linked to iron metabolism (*tfr1a*, possibly a transferrin receptor) was significantly upregulated by pyrene and phenanthrene after 7 days of exposure, with a higher fold change for the former (Supplementary file 2). Most of the over-represented KEGG or Reactome pathways terms were linked to the metabolism of xenobiotics (data not shown). The Reactome pathway muscle contraction (R-DRE-397014) was over-represented for 3 days of exposure to retene and included in the figure 5, as it was featuring

a couple of genes not involved in the related over-represented GO terms (i.e. *cacng8b* and *mylpfa*).

4. Discussion

4.1. PAHs caused almost no detectable deformities or growth retardation

The present study aimed to focus on sublethal effects of the three tested individual PAHs, and none of the tested concentrations significantly altered the mortality, body length or yolk sac area of the rainbow trout larvae at any time point. Similar results have been reported for retene using the same exposure concentration (32 µg.L^{-1}), fish species and similar experimental designs (Billiard et al., 1999; Vehniäinen et al., 2016). To our knowledge, there is very little literature regarding the embryotoxicity of pyrene and phenanthrene in rainbow trout or in other salmonids species. Koskinen et al. (2004) reported no significant increase in mortality in rainbow trout larvae exposed to 100 µg.L^{-1} of pyrene, however the fish were exposed 10 days after hatch. Hawkins et al. (2002) reported a relatively high mortality (36%) and a significant increase in the prevalence of yolk sac edemas (9%) and craniofacial deformities (100%) in rainbow trout larvae exposed to a similar concentration of phenanthrene (100 µg.L^{-1}). However, these effects were measured after 22 days of exposure. The longer exposure (8 days more than our longest exposure) may explain the difference with our study. Effects on survival, growth or deformity index were observed for pyrene and phenanthrene in other various fish species ELS at concentrations ranging from 20 to 200 µg.L^{-1} (Hendon et al., 2008; Mu et al., 2012; Sugahara et al., 2014). However, possible differences in species sensitivity to PAHs, toxicokinetics, life stages and more generally experimental designs makes the comparison among those different studies and the present one quite difficult.

4.2. Concentrations of PAHs in larvae and exposure water

Even in the absence of larvae, the measured concentrations of retene, pyrene and phenanthrene in the exposure water were 3 to 4 times lower than the nominal concentrations of the experiment (Fig. 1A). PAHs are hydrophobic compounds, thus it is likely that a portion of the PAHs added in the exposure water are adsorbed by the glass walls of the exposure tanks (Qian et al., 2011), or by the DOC of the lake water. In order to minimize the impact of this factor on the fish exposures, the tanks were prepared one day before the beginning of the experiment to saturate the glass walls with the PAHs. Additionally, microorganisms that are naturally present in the lake water used as an exposure medium can contribute to PAHs degradation (Mrozik et al., 2003). PAHs are also readily metabolized by fish. Due to these factors, it is very likely that the actual exposure concentrations for the fish were overall much lower than the nominal concentrations. By providing both the concentrations of the parent PAHs in the water before the daily renewal and in the fish tissues at the end of each exposure, we aimed to provide enough information to make the present work as comparable as possible with previous and future studies.

In the presence of larvae, the concentrations of retene and pyrene measured in the water tended to decrease over time, while no particular trend was observed for phenanthrene (Fig. 1A). For retene, similar observations for waterborne exposures involving rainbow trout larvae have been reported before (Billiard et al., 1999; Scott and Hodson, 2008; Scott et al., 2009; Vehniäinen et al., 2016). Retene levels in the larvae were very low (close to background levels) at the end of the different exposures (Fig. 2), which is similar to the result reported by Hodson et al. (2007) in rainbow trout larvae exposed to retene only. On the other hand, phenanthrene levels in larvae were higher at the end of the exposures, and did not show any particular trend over time (Fig. 2).

Based on those observations, we can assume that retene is effectively metabolized by rainbow trout larvae, while phenanthrene is degraded more slowly and remains for a longer period in their body. Another possible hypothesis is that those compounds are taken up more or less efficiently by the larvae. Pyrene was found at a noticeably higher concentration than retene in the larvae (Fig. 2), suggesting that it might also be metabolized less efficiently than retene. Overall, those assumptions match well with the respective known affinities of those PAHs with the AhR in fish (Barron et al., 2004) as well as their measured levels of cytochrome P4501A induction at the mRNA level (Supplementary file 2).

4.3. Key cardiac genes are altered by retene and pyrene

At the tested concentrations, retene appeared to be the most potent of the three PAHs in terms of DEGs, with the highest number of altered genes being recorded after 1 and 3 days of exposure (Fig. 3). A similar trend over time was observed by Vehniäinen et al. (2016) for retene in the cardiac transcriptome of the rainbow trout larvae, in a very similar experimental setup but using a different microarray design. Pyrene also appeared to be more potent during early development, with a very high number of DEGs being observed after 1 day of exposure compared to the other sampling time points (Fig. 3). This temporal trend may be explained by several factors such as the rapid development of the embryos, the declining water concentrations of retene and pyrene as well as their cumulative toxicity over time (Vehniäinen et al., 2016). At longer exposure times, the cardiac tissue may also have been exposed to increasing concentrations of retene and pyrene metabolites that interfere with the parent compounds. In comparison to the two AhR agonists, phenanthrene appeared not very potent to cause transcriptomic changes. By using RNA sequencing to study the effects of several PAHs on the zebrafish ELS transcriptome, Shankar et al. (2019) found that retene was almost ten times more potent than phenanthrene to induce

changes in the transcriptome. Overall, the DEGs trends were quite well translated into the ORAs outputs, with the highest number of over-represented GO terms being found for retene and the lowest for phenanthrene (Fig. 4).

Among the genes altered by retene that were linked to cation transport or muscle contraction, several were related to key cardiac ion channels. The principal role of those cardiac ion channels is to generate the cardiac action potential (AP) responsible for the contraction of the heart. Each of the different functional parts of the heart has specific electrophysiological characteristics and thus different ion channel compositions (Vornanen, 2017). Besides their electrophysiological functions in the heart, ion channels are also involved in heart development and morphogenesis (Keßler et al., 2012). In this study, retene significantly upregulated *cacng8b*, one subunit of an L-type Ca^{2+} channel, after 3 days of exposure. At the same time point, retene also downregulated the expression of the *casq1b* gene, encoding for one isoform of calsequestrin, a protein involved in the storage of calcium into the sarcoplasmic reticulum of cardiomyocytes (Györke et al., 2009). Retene also significantly downregulated the expression of *atp2a1l* and *slc24a2* after respectively 3 and 14 days of exposure (Supplementary file 2). The former encodes for one subunit of the SERCA (sarco/endoplasmic reticulum Ca^{2+}-ATPase) pump responsible for pumping the cytoplasmic calcium back into the sarcoplasmic reticulum, while the latter encodes for one subunit of the NCKX exchanger, a sodium/calcium/potassium exchanger. Calcium homeostasis is known to be a target of complex PAH mixtures in fish (Greer et al., 2019; Xu et al., 2016; Xu et al., 2019). Our results suggest that retene alone is potentially able to disrupt calcium homeostasis and storage in cardiac cells. This is further supported by the fact that several DEGs encoding for proteins involved in calcium handling (among them cadherin, several

calpains and parvalbumins) were altered by retene at some point without showing up in the ORAs: *cdh11*, *capn9*, *capn12*, *pvalb2*, *pvalb4*, *pvalb2* and *s100a11* (Supplementary file 2).

Calcium was not the only ion affected by retene, and several genes encoding for subunits of the Na^+/K^+ pump were downregulated after 1 day of exposure: *atp1a1a.1*, *atp1a1a.4* and *atp1b1b*. The Na^+/K^+ pump regulates the intracellular Na^+ homeostasis. In the zebrafish embryo, blocking the α1B1 isoform of the Na^+/K^+ pump by pharmacological means or by morpholino oligonucleotides caused several cardiovascular defects such as pericardial edemas, abnormal heart tube elongation, aberrant cardiomyocyte differentiation, and reduced heart rate and contractility (Shu et al., 2003). Two genes related to two different subunits of two different types of K^+ channels were also altered by retene after 1 or 3 days of exposure: *kcnj1a.1* (downregulation, Fig. 5) and *kcnc3a* (upregulation, Supplementary file 2). In the zebrafish larvae, the morpholino knockdown of *kcnj1* resulted in an increase of the heart rate (Abbas et al., 2011).

Compared to retene, pyrene only affected a few genes potentially involved in the generation of the AP: *cacna1i*, *kcna10a*, *kcnh8* and *kcnj9* (Supplementary file 2). All those genes were significantly altered after one day of exposure. *cacna1i* encodes for one subunit of a T-type Ca^{2+} channel. While the pacemaking role of T-type Ca^{2+} channels is well established in mammals, birds and frogs, it is less clear in fish and remains to be functionally and molecularly characterized (Mangoni et al., 2006; Vornanen, 2017). Finally, phenanthrene was only affecting one AP-related ion channel: *cacng7a* was found to be significantly upregulated after one day of exposure (Supplementary file 2). Similar to *cacng8b* (which was upregulated by retene), *cacng7a* encodes for one subunit of an L-type Ca^{2+} channel.

In the present study, retene also altered the expression of several genes related to actin filaments (*fscn2b* and *actn3b*), myosin filaments (*myha*, *myhc4*, *myhz1.1*, *myhz1.2* and *myhz2*) and the troponin complex (*tnni1c*, *tnni2a.4*, *tnnt1* and *tpma*) after 3 days of exposure. If the correct generation and propagation of the cardiac AP is a required condition for a normal cardiac rhythm and contraction, another important parameter is the proper formation of the cardiac muscles, i.e. the correct formation of the sarcomeres. Sarcomeres are composed mostly of two important groups of protein, actins and myosins. A third group of protein, troponins, forms the troponin complex, which is attached to the surface of the sarcomeres. Following propagation of the cardiac AP and the increased concentration of Ca^{2+} in the myocyte, the troponin complex will bind with calcium ions and trigger muscle contraction. Retene was previously shown to alter several genes involved in the organization of actin filaments in the rainbow trout ELS, although without any mention of genes related to myosin or the troponin complex (Vehniäinen et al., 2016). Potent AhR agonists such as the model dioxin 2,3,7,8-tetrachlorodibenzo-*p*-dioxin (TCDD) and coplanar polychlorinated biphenyls (PCBs) are also known to alter the expression of several genes related to actin, myosin and troponin in various fish species (Carlson et al., 2009; Handley-Goldstone et al., 2005; Iida et al., 2016). Similar observations have been made *in vitro* in mouse cardiomyocytes exposed to TCDD (Neri et al., 2011; Wang et al., 2009).

Pyrene, on the other hand, only altered the expression of all the aforementioned myosin isoforms affected by retene, in addition to *mybpc1* and *myh10*, after 1 day of exposure (Fig. 6), as well as one gene related to actin, *actb2* (Supplementary file 2, upregulated after 1 day). However, while retene mostly downregulated those myosin-related genes, pyrene had the opposite effect (except for *myh10*). It is also worth mentioning that all the tested PAHs significantly reduced the expression of *tnnt2a* (troponin T type 2a, cardiac) after 7 days of exposure (Supplementary file

2). Troponin T is an essential component of cardiac contraction in the zebrafish heart (Sehnert et al., 2002). Interestingly, the morpholino knockdown of the gene encoding for troponin T caused symptoms similar to phenanthrene in the zebrafish embryo, i.e. curved tails, pericardial and yolk sac edemas (Incardona et al., 2004). The present study suggests that retene and pyrene could contribute to those symptoms by affecting the expression of troponin T as well.

The present study did not investigate the long-term effects of an early exposure to PAHs on the later development of the fish, thus discussing this aspect based on our own data would be purely speculative. Exposure to environmentally relevant concentrations of crude oil during embryogenesis caused a loss in cardiac fitness in juveniles Pacific herring (*Clupea pallasi*) and pink salmon (*Oncorhynchus gorbuscha*) several months after exposure (Incardona et al., 2015). Similar findings were also described in the zebrafish (Hicken et al., 2011). However, to our knowledge, there are no studies linking the effects on the cardiac transcriptome of an exposure to PAHs at the larval stage to the later cardiac function nor the general development of the juvenile or adult fish. Exposures with similar concentrations of retene, pyrene and phenanthrene are currently underway to assess their effects on the cardiac function of the rainbow trout larvae.

4.4. Other notable effects of PAHs on the cardiac transcriptome

Pyrene altered several genes linked with the respiratory electron transport chain (RETC), oxygen binding or iron binding after 14 days of exposure (Fig. 6). *sdha* and *sdhb* (succinate dehydrogenase [ubiquinone] flavoprotein and iron-sulfur subunits, respectively) are linked to two subunits of the succinate dehydrogenase enzymatic complex of the mitochondria, a key component of the RETC. *cycsb* (cytochrome c, somatic b), which bind with heme complexes in the mitochondria, also participates to this process and was significantly upregulated by pyrene after 7 days of exposure (Supplementary file 2). Mitochondrial respiration has already been

shown to be altered by PAHs alone or in mixtures (Lindberg and Di Giulio, 2019; Raftery et al., 2017), but the present study is to our knowledge the first one to mention pyrene in that regard. Genes related to the hemoglobin complex or iron metabolism (possibly ferritin and transferrin) were also altered by pyrene in the cardiac tissue of the rainbow trout ELS (Fig. 6 and Supplementary file 2). Pyrene has been shown to alter genes involved in iron homeostasis in the liver of the juvenile rainbow trout (Krasnov et al., 2005). Taken together, these observations suggest that pyrene may disrupt the RETC and the metabolism of iron, two processes that are essential to provide the energy and the proper metabolism of oxygen for the cardiac function. Phenanthrene appeared to alter the expression of the same genes linked to oxygen binding and iron binding, but not to the RETC (Fig. 6).

All three PAHs altered the expression of several genes involved in the regulation of transcription, cell differentiation and more generally multicellular organism development (Supplementary file 2): retene appeared once again as the most potent of the three tested PAHs, with several homeobox, FOX and SOX genes being significantly downregulated after one day of exposure. Pyrene and phenanthrene affected less genes than retene, and only *sox21b* and *dlx4a* were common to all three PAHs at any given time point. Alteration in the expression of genes related to transcription and cell differentiation is a common response following exposure to model AhR agonists (Carney et al., 2006; Chen et al., 2008) and was already described in the rainbow trout heart for retene (Vehniäinen et al., 2016). Our data suggests that weaker AhR agonists such as pyrene and phenanthrene can also affect similar genes, but with less potency.

In the present study, phenanthrene induced very few DEGs compared to retene or pyrene. Phenanthrene induction of *cyp1a* was not significant after one day of exposure but increased to levels comparable to those of pyrene after 3 days of exposure and later. Induction of CYP1A

enzymes by phenanthrene has been observed before by immunofluorescence in the zebrafish ELS (Incardona et al., 2005), for example. However, despite similar AhR activation levels between pyrene and phenanthrene after 3 days of exposure and later, almost no overlap of DEGs were observed for those two compounds. One notable effect of phenanthrene compared to the two other PAHs tested was its ability to alter the expression of several genes linked to collagens or related proteins, such as fibronectins (Supplementary file 2). Altered collagen content following exposure to phenanthrene was observed in the developing zebrafish heart by Zhang et al. (2013). The authors speculated that this effect could result from the direct or indirect activation of MMP-9 (matrix metalloproteinase-9, a collagenase) by phenanthrene. In the present study, no gene linked to matrix metalloproteinase was found to be altered by any of the tested PAHs. However, both pyrene and phenanthrene significantly downregulated the expression of *lum* (lumican) after 7 days of exposure (Supplementary file 2). Interestingly, lumican inhibits of the activity of at least one matrix metalloproteinase isoform (MMP-14) in mammalian cells (Pietraszek et al., 2014).

5. Conclusion

The three widespread model PAHs retene, pyrene and phenanthrene were all able to induce significant and compound-specific changes in the cardiac transcriptome of the rainbow trout ELS. Our findings for retene are consistent with the existing literature and further strengthen its role as a potent disruptor of the cardiac function at the molecular level, from the generation of the action potential to muscle contraction. Pyrene and phenanthrene appeared less potent to induce changes in genes related to those processes, and pyrene had opposite effects compared to retene in regards to several myosin-related genes, suggesting once again compound-specific mechanisms of toxicity. Pyrene and to a lesser extent phenanthrene altered key genes linked to

the respiratory electron transport chain, as well as to oxygen and iron metabolism. Overall, phenanthrene appeared relatively inefficient at inducing significant changes in the cardiac transcriptome compared to retene and pyrene. This observation can however appear contradictory with its ability to induce the AhR as potently as pyrene, as well as with its apparent slower metabolism compared to both retene and pyrene. One explanation could be that phenanthrene is capable of disrupting the cardiac function via other mechanisms that modulates directly the ion currents and the action potential (Vehniäinen et al., 2019). More research is currently underway to better understand the effects of those compounds (alone or in mixtures) on the cardiac function of the rainbow trout ELS, as well as the toxicokinetics parameters that lies behind.

Acknowledgements

The present study was funded by the Academy of Finland (projects 285296, 294066 and 319284 to Eeva-Riikka Vehniäinen). The authors are grateful to Mervi Koistinen, Terhi Rahkonen, Jaakko Litmanen as well as the personnel of the Konnevesi Research Station for their technical assistance. We also thank Gerrit Timmerhaus for his precious help during the preparation of the microarrays.

Data accessibility statement

The microarray data have been deposited in the ArrayExpress database at EMBL-EBI under accession number E-MTAB-8750.

REFERENCES

Abbas L, Hajihashemi S, Stead LF, Cooper GJ, Ware TL, Munsey TS, Whitfield TT, White SJ, 2011. Functional and developmental expression of a zebrafish Kir1.1 (ROMK) potassium channel homologue Kcnj1. J Physiol (Lond). 589, 1489-503.

Ahad JM, Jautzy JJ, Cumming BF, Das B, Laird KR, Sanei H, 2015. Sources of polycyclic aromatic hydrocarbons (PAHs) to northwestern Saskatchewan lakes east of the Athabasca oil sands. Org Geochem. 80, 35-45.

Ainerua MO, Tinwell J, Kompella SN, Sørhus E, White KN, van Dongen BE, Shiels HA, 2020. Understanding the cardiac toxicity of the anthropogenic pollutant phenanthrene on the freshwater indicator species, the brown trout (*Salmo trutta*): From whole heart to cardiomyocytes. Chemosphere. 239, 124608.

Anyakora C, Ogbeche A, Palmer P, Coker H, 2005. Determination of polynuclear aromatic hydrocarbons in marine samples of Siokolo Fishing Settlement. Journal of chromatography A. 1073, 323-30.

Ashburner M, Ball CA, Blake JA, Botstein D, Butler H, Cherry JM, Davis AP, Dolinski K, Dwight SS, Eppig JT, 2000. Gene ontology: tool for the unification of biology. Nat Genet. 25, 25.

Bak S, Nakata H, Koh D, Yoo J, Iwata H, Kim E, 2019. In vitro and in silico AHR assays for assessing the risk of heavy oil-derived polycyclic aromatic hydrocarbons in fish. Ecotoxicol Environ Saf. 181, 214-23.

Barron MG, Heintz R, Rice SD, 2004. Relative potency of PAHs and heterocycles as aryl hydrocarbon receptor agonists in fish. Marine Environmental Research. 58, 95-100.

Benjamini Y, Hochberg Y, 1995. Controlling the false discovery rate: a practical and powerful approach to multiple testing. Journal of the Royal statistical society: series B (Methodological). 57, 289-300.

Billiard SM, Meyer JN, Wassenberg DM, Hodson PV, Di Giulio R,T., 2008. Nonadditive effects of PAHs on early vertebrate development: mechanisms and implications for risk assessment. Toxicological Sciences. 105, 5-23.

Billiard SM, Querbach K, Hodson PV, 1999. Toxicity of retene to early life stages of two freshwater fish species. Environmental Toxicology and Chemistry: An International Journal. 18, 2070-7.

Boyle EI, Weng S, Gollub J, Jin H, Botstein D, Cherry JM, Sherlock G, 2004. GO::TermFinder—open source software for accessing Gene Ontology information and finding significantly enriched Gene Ontology terms associated with a list of genes. Bioinformatics. 20, 3710-5.

Brette F, Shiels HA, Galli GLJ, Cros C, Incardona JP, Scholz NL, Block BA, 2017. A novel cardiotoxic mechanism for a pervasive global pollutant. Scientific reports. 7, 41476.

Brinkworth LC, Hodson PV, Tabash S, Lee P, 2003. CYP1A induction and blue sac disease in early developmental stages of rainbow trout (*Oncorhynchus mykiss*) exposed to retene. Journal of Toxicology and Environmental Health, Part A. 66, 627-46.

Carlson EA, Roy NK, Wirgin II, 2009. Microarray analysis of polychlorinated biphenyl mixture–induced changes in gene expression among Atlantic tomcod populations displaying differential sensitivity to halogenated aromatic hydrocarbons. Environmental Toxicology and Chemistry: An International Journal. 28, 759-71.

Carney SA, Chen J, Burns CG, Xiong KM, Peterson RE, Heideman W, 2006. Aryl hydrocarbon receptor activation produces heart-specific transcriptional and toxic responses in developing zebrafish. Mol Pharmacol. 70, 549-61.

Chen J, Carney SA, Peterson RE, Heideman W, 2008. Comparative genomics identifies genes mediating cardiotoxicity in the embryonic zebrafish heart. Physiological genomics. 33, 148-58.

Cypher AD, Consiglio J, Bagatto B, 2017. Hypoxia exacerbates the cardiotoxic effect of the polycyclic aromatic hydrocarbon, phenanthrene in *Danio rerio*. Chemosphere. 183, 574-81.

Doering J, Hecker M, Villeneuve D, Zhang X, 2019. Adverse Outcome Pathway on aryl hydrocarbon receptor activation leading to early life stage mortality, via increased COX-2.

Greer JB, Pasparakis C, Stieglitz JD, Benetti D, Grosell M, Schlenk D, 2019. Effects of corexit 9500A and Corexit-crude oil mixtures on transcriptomic pathways and developmental toxicity in early life stage mahi-mahi (*Coryphaena hippurus*). Aquatic Toxicology. 212, 233-40.

Györke S, Stevens SCW, Terentyev D, 2009. Cardiac calsequestrin: quest inside the SR. J Physiol (Lond). 587, 3091-4.

Handley-Goldstone HM, Grow MW, Stegeman JJ, 2005. Cardiovascular gene expression profiles of dioxin exposure in zebrafish embryos. Toxicological Sciences. 85, 683-93.

Hawkins SA, Billiard SM, Tabash SP, Brown RS, Hodson PV, 2002. Altering cytochrome P4501A activity affects polycyclic aromatic hydrocarbon metabolism and toxicity in rainbow trout (*Oncorhynchus mykiss*). Environmental Toxicology and Chemistry: An International Journal. 21, 1845-53.

He C, Zuo Z, Shi X, Sun L, Wang C, 2012. Pyrene exposure influences the thyroid development of *Sebastiscus marmoratus* embryos. Aquatic toxicology. 124, 28-33.

Hendon LA, Carlson EA, Manning S, Brouwer M, 2008. Molecular and developmental effects of exposure to pyrene in the early life-stages of *Cyprinodon variegatus*. Comparative Biochemistry and Physiology Part C: Toxicology & Pharmacology. 147, 205-15.

Hicken CE, Linbo TL, Baldwin DH, Willis ML, Myers MS, Holland L, Larsen M, Stekoll MS, Rice SD, Collier TK, 2011. Sublethal exposure to crude oil during embryonic development alters

cardiac morphology and reduces aerobic capacity in adult fish. Proceedings of the National Academy of Sciences. 108, 7086-90.

Hodson PV, 2017. The toxicity to fish embryos of PAH in crude and refined oils. Arch Environ Contam Toxicol. 73, 12-8.

Hodson PV, Qureshi K, Noble CAJ, Akhtar P, Brown RS, 2007. Inhibition of CYP1A enzymes by α-naphthoflavone causes both synergism and antagonism of retene toxicity to rainbow trout (*Oncorhynchus mykiss*). Aquatic toxicology. 81, 275-85.

Honkanen JO, Rees CB, Kukkonen JV, Hodson PV, 2020. Temperature determines the rate at which retene affects trout embryos, not the concentration that is toxic. Aquatic Toxicology, 105471.

Iida M, Fujii S, Uchida M, Nakamura H, Kagami Y, Agusa T, Hirano M, Bak S, Kim E, Iwata H, 2016. Identification of aryl hydrocarbon receptor signaling pathways altered in TCDD-treated red seabream embryos by transcriptome analysis. Aquatic Toxicology. 177, 156-70.

Incardona JP, Carls MG, Hiroki T, Sloan CA, Collier TK, Scholz NL, 2005. Aryl hydrocarbon receptor–independent toxicity of weathered crude oil during fish development. Environ Health Perspect. 113, 1755-62.

Incardona JP, Carls MG, Holland L, Linbo TL, Baldwin DH, Myers MS, Peck KA, Tagal M, Rice SD, Scholz NL, 2015. Very low embryonic crude oil exposures cause lasting cardiac defects in salmon and herring. Scientific Reports. 5, 13499.

Incardona JP, Collier TK, Scholz NL, 2004. Defects in cardiac function precede morphological abnormalities in fish embryos exposed to polycyclic aromatic hydrocarbons. Toxicology and Applied Pharmacology. 196, 191-205.

Incardona JP, Day HL, Collier TK, Scholz NL, 2006. Developmental toxicity of 4-ring polycyclic aromatic hydrocarbons in zebrafish is differentially dependent on AH receptor isoforms and hepatic cytochrome P4501A metabolism. Toxicology and Applied Pharmacology. 217, 308-21.

Jung J, Kim M, Yim UH, Ha SY, Shim WJ, Chae YS, Kim H, Incardona JP, Linbo TL, Kwon J, 2015. Differential toxicokinetics determines the sensitivity of two marine embryonic fish exposed to Iranian Heavy Crude Oil. Environ Sci Technol. 49, 13639-48.

Kamler E, 2002. Ontogeny of yolk-feeding fish: an ecological perspective. Rev Fish Biol Fish. 12, 79-103.

Keßler M, Just S, Rottbauer W, 2012. Ion flux dependent and independent functions of ion channels in the vertebrate heart: lessons learned from zebrafish. Stem cells international. 2012.

Koskinen H, Pehkonen P, Vehniäinen E, Krasnov A, Rexroad C, Afanasyev S, Mölsa H, Oikari A, 2004. Response of rainbow trout transcriptome to model chemical contaminants. Biochem Biophys Res Commun. 320, 745-53.

Krasnov A, Koskinen H, Rexroad C, Afanasyev S, Mölsä H, Oikari A, 2005. Transcriptome responses to carbon tetrachloride and pyrene in the kidney and liver of juvenile rainbow trout (*Oncorhynchus mykiss*). Aquatic Toxicology. 74, 70-81.

Krasnov A, Timmerhaus G, Afanasyev S, Jørgensen SM, 2011. Development and assessment of oligonucleotide microarrays for Atlantic salmon (*Salmo salar* L.). Comparative Biochemistry and Physiology Part D: Genomics and Proteomics. 6, 31-8.

Kurek J, Kirk JL, Muir DC, Wang X, Evans MS, Smol JP, 2013. Legacy of a half century of Athabasca oil sands development recorded by lake ecosystems. Proceedings of the National Academy of Sciences. 110, 1761-6.

Larigot L, Juricek L, Dairou J, Coumoul X, 2018. AhR signaling pathways and regulatory functions. Biochimie open. 7, 1-9.

Latimer JS, Zheng J. The sources, transport, and fate of PAHs in the marine environment. In: Douben PET, editor. PAHs: An Ecotoxicological Perspective; 2003. p. 7-33.

Le Bihanic F, Clérandeau C, Le Menach K, Morin B, Budzinski H, Cousin X, Cachot J, 2014. Developmental toxicity of PAH mixtures in fish early life stages. Part II: adverse effects in Japanese medaka. Environmental Science and Pollution Research. 21, 13732-43.

Leppänen H, Oikari A, 2001. Retene and resin acid concentrations in sediment profiles of a lake recovering from exposure to pulp mill effluents. J Paleolimnol. 25, 367-74.

Lindberg CD, Di Giulio RT, 2019. Polycyclic aromatic hydrocarbon and hypoxia exposures result in mitochondrial dysfunction in zebrafish. Aquatic Toxicology. 216, 105298.

Logan DT, 2007. Perspective on ecotoxicology of PAHs to fish. Human and Ecological Risk Assessment: An International Journal. 13, 302-16.

Madison BN, Hodson PV, Langlois VS, 2015. Diluted bitumen causes deformities and molecular responses indicative of oxidative stress in Japanese medaka embryos. Aquatic Toxicology. 165, 222-30.

Mangoni ME, Couette B, Marger L, Bourinet E, Striessnig J, Nargeot J, 2006. Voltage-dependent calcium channels and cardiac pacemaker activity: from ionic currents to genes. Prog Biophys Mol Biol. 90, 38-63.

Maskaoui K, Zhou JL, Hong HS, Zhang ZL, 2002. Contamination by polycyclic aromatic hydrocarbons in the Jiulong River estuary and Western Xiamen Sea, China. Environmental pollution. 118, 109-22.

Meriläinen P, Lahdelma I, Oikari L, Hyötyläinen T, Oikari A, 2006. Dissolution of resin acids, retene and wood sterols from contaminated lake sediments. Chemosphere. 65, 840-6.

Mrozik A, Piotrowska-Seget Z, Labuzek S, 2003. Bacterial degradation and bioremediation of polycyclic aromatic hydrocarbons. Polish Journal of Environmental Studies. 12, 15-25.

Mu J, Wang J, Jin F, Wang X, Hong H, 2014. Comparative embryotoxicity of phenanthrene and alkyl-phenanthrene to marine medaka (*Oryzias melastigma*). Marine Pollution Bulletin. 85, 505-15.

Mu J, Wang X, Jin F, Wang J, Hong H, 2012. The role of cytochrome P4501A activity inhibition in three-to five-ringed polycyclic aromatic hydrocarbons embryotoxicity of marine medaka (*Oryzias melastigma*). Mar Pollut Bull. 64, 1445-51.

Neri T, Merico V, Fiordaliso F, Salio M, Rebuzzini P, Sacchi L, Bellazzi R, Redi CA, Zuccotti M, Garagna S, 2011. The differentiation of cardiomyocytes from mouse embryonic stem cells is altered by dioxin. Toxicol Lett. 202, 226-36.

Pietraszek K, Chatron-Colliet A, Brézillon S, Perreau C, Jakubiak-Augustyn A, Krotkiewski H, Maquart F, Wegrowski Y, 2014. Lumican: A new inhibitor of matrix metalloproteinase-14 activity. FEBS Lett. 588, 4319-24.

Qian Y, Posch T, Schmidt TC, 2011. Sorption of polycyclic aromatic hydrocarbons (PAHs) on glass surfaces. Chemosphere. 82, 859-65.

Raftery TD, Jayasundara N, Di Giulio RT, 2017. A bioenergetics assay for studying the effects of environmental stressors on mitochondrial function in vivo in zebrafish larvae. Comparative Biochemistry and Physiology Part C: Toxicology & Pharmacology. 192, 23-32.

Rueden CT, Schindelin J, Hiner MC, DeZonia BE, Walter AE, Arena ET, Eliceiri KW, 2017. ImageJ2: ImageJ for the next generation of scientific image data. BMC Bioinformatics. 18, 529.

Ruge Z, Muir D, Helm P, Lohmann R, 2015. Concentrations, trends, and air-water exchange of PAHs and PBDEs derived from passive samplers in Lake Superior in 2011. Environ Sci Technol. 49, 13777-86.

Scott JA, Hodson PV, 2008. Evidence for multiple mechanisms of toxicity in larval rainbow trout (*Oncorhynchus mykiss*) co-treated with retene and α-naphthoflavone. Aquatic toxicology. 88, 200-6.

Scott JA, Incardona JP, Pelkki K, Shepardson S, Hodson PV, 2011. AhR2-mediated, CYP1A-independent cardiovascular toxicity in zebrafish (*Danio rerio*) embryos exposed to retene. Aquatic Toxicology. 101, 165-74.

Scott JA, Ross M, Lemire BC, Hodson PV, 2009. Embryotoxicity of retene in cotreatment with 2-aminoanthracene, a cytochrome P4501A inhibitor, in rainbow trout (*Oncorhynchus mykiss*). Environmental toxicology and chemistry. 28, 1304-10.

Sehnert AJ, Huq A, Weinstein BM, Walker C, Fishman M, Stainier DY, 2002. Cardiac troponin T is essential in sarcomere assembly and cardiac contractility. Nat Genet. 31, 106.

Shankar P, Geier MC, Truong L, McClure RS, Pande P, Waters KM, Tanguay RL, 2019. Coupling genome-wide transcriptomics and developmental toxicity profiles in zebrafish to characterize polycyclic aromatic hydrocarbon (PAH) hazard. International journal of molecular sciences. 20, 2570.

Shen G, Tao S, Wei S, Zhang Y, Wang R, Wang B, Li W, Shen H, Huang Y, Yang Y, 2012. Retene emission from residential solid fuels in China and evaluation of retene as a unique marker for soft wood combustion. Environ Sci Technol. 46, 4666-72.

Shi X, He C, Zuo Z, Li R, Chen D, Chen R, Wang C, 2012. Pyrene exposure influences the craniofacial cartilage development of *Sebastiscus marmoratus* embryos. Mar Environ Res. 77, 30-4.

Shu X, Cheng K, Patel N, Chen F, Joseph E, Tsai H, Chen J, 2003. Na, K-ATPase is essential for embryonic heart development in the zebrafish. Development. 130, 6165-73.

Sugahara Y, Kawaguchi M, Itoyama T, Kurokawa D, Tosa Y, Kitamura S, Handoh IC, Nakayama K, Murakami Y, 2014. Pyrene induces a reduction in midbrain size and abnormal swimming behavior in early-hatched pufferfish larvae. Mar Pollut Bull. 85, 479-86.

Sun L, Zuo Z, Chen M, Chen Y, Wang C, 2015. Reproductive and transgenerational toxicities of phenanthrene on female marine medaka (*Oryzias melastigma*). Aquatic Toxicology. 162, 109-16.

Tabash SP, 2003. An investigation of the metabolism of alkyl substituted polycyclic aromatic hydrocarbons by cytochrome P450 enzymes.

Turcotte D, Akhtar P, Bowerman M, Kiparissis Y, Brown RS, Hodson PV, 2011. Measuring the toxicity of alkyl-phenanthrenes to early life stages of medaka (Oryzias latipes) using partition-controlled delivery. Environmental Toxicology and Chemistry. 30, 487-95.

Vehniäinen E, Bremer K, Scott JA, Junttila S, Laiho A, Gyenesei A, Hodson PV, Oikari AOJ, 2016. Retene causes multifunctional transcriptomic changes in the heart of rainbow trout (*Oncorhynchus mykiss*) embryos. Environ Toxicol Pharmacol. 41, 95-102.

Vehniäinen E, Haverinen J, Vornanen M, 2019. Polycyclic aromatic hydrocarbons phenanthrene and retene modify the action potential via multiple ion currents in rainbow trout *Oncorhynchus mykiss* cardiac myocytes. Environ Toxicol Chem. 0.

Villalobos SA, Papoulias DM, Meadows J, Blankenship AL, Pastva SD, Kannan K, Hinton DE, Tillitt DE, Giesy JP, 2000. Toxic responses of medaka, d-rR strain, to polychlorinatednaphthalene mixtures after embryonic exposure by in ovo nanoinjection: A partial life-cycle assessment. Environmental toxicology and chemistry. 19, 432-40.

Vornanen M, 2017. Electrical excitability of the fish heart and its autonomic regulation. Fish Physiology. 36, 99-153.

Wang Y, Fan Y, Puga A, 2009. Dioxin exposure disrupts the differentiation of mouse embryonic stem cells into cardiomyocytes. Toxicological sciences. 115, 225-37.

Watson GM, Andersen O, Galloway TS, Depledge MH, 2004. Rapid assessment of polycyclic aromatic hydrocarbon (PAH) exposure in decapod crustaceans by fluorimetric analysis of urine and haemolymph. Aquatic toxicology. 67, 127-42.

Wolska L, Mechlińska A, Rogowska J, Namieśnik J, 2012. Sources and fate of PAHs and PCBs in the marine environment. Crit Rev Environ Sci Technol. 42, 1172-89.

Xu EG, Khursigara AJ, Li S, Esbaugh AJ, Dasgupta S, Volz DC, Schlenk D, 2019. mRNA-miRNA-Seq reveals neuro-cardio mechanisms of crude oil toxicity in red drum (*Sciaenops ocellatus*). Environ Sci Technol. 53, 3296-305.

Xu EG, Mager EM, Grosell M, Pasparakis C, Schlenker LS, Stieglitz JD, Benetti D, Hazard ES, Courtney SM, Diamante G, 2016. Time-and oil-dependent transcriptomic and physiological responses to Deepwater Horizon oil in mahi-mahi (*Coryphaena hippurus*) embryos and larvae. Environ Sci Technol. 50, 7842-51.

Yu G, Wang L, Han Y, He Q, 2012. clusterProfiler: an R package for comparing biological themes among gene clusters. Omics: a journal of integrative biology. 16, 284-7.

Zhang Y, Huang L, Wang C, Gao D, Zuo Z, 2013. Phenanthrene exposure produces cardiac defects during embryo development of zebrafish (*Danio rerio*) through activation of MMP-9. Chemosphere. 93, 1168-75.

Zhang Y, Huang L, Zuo Z, Chen Y, Wang C, 2013. Phenanthrene exposure causes cardiac arrhythmia in embryonic zebrafish via perturbing calcium handling. Aquatic Toxicology. 142-143, 26-32.

Zhang Y, Wang C, Huang L, Chen R, Chen Y, Zuo Z, 2012. Low-level pyrene exposure causes cardiac toxicity in zebrafish (*Danio rerio*) embryos. Aquatic toxicology. 114, 119-24.

FIGURE AND TABLE CAPTIONS

Fig. 1. (A) Boxplots of the concentrations ($\mu g.L^{-1}$) of retene, pyrene and phenanthrene measured in water by SFS after 1, 3, 7, 10 or 14 days of exposure (N = 4-20) or in tanks without fish (N = 8-9). **(B)** Average fluorescence spectrums for pyrene in the exposure water after 1, 3, 7, 10 or 14 days (N = 4-20), and in tanks without fish (N = 9).

Fig. 2. Boxplots of the average retene (A), pyrene (B) or phenanthrene (C) content per larva (ng per larva) measured by HPLC after 1, 3, 7 or 14 days of exposure (N = 8).

Fig. 3. Venn diagrams showing unique and shared gene expression (DEGs compared to controls) in the hearts of rainbow trout larvae after 1, 3, 7 or 14 days (diagrams A, B, C and D respectively) of exposure to retene, pyrene or phenanthrene. Numbers represent the number of genes downregulated or upregulated, respectively.

Fig. 4. Overview of the over-representation analyzes (ORAs) results showing the significantly over-represented GO terms in the gene expression dataset. ORAs are based on the gene expression dataset (DEGs compared to controls) after that a zebrafish (*Danio rerio*) RefSeq gene ID and gene symbol was attributed to each feature of the microarray. RET, PYR and PHE are standing for retene, pyrene and phenanthrene, respectively. The numbers that follows RET, PYR or PHE are standing for the sampling day (1, 3, 7 or 14 days).

Fig. 5. Heat maps of the ORAs output for retene (32 $\mu g.L^{-1}$) after 1, 3, 7 or 14 days of exposure (shortened as RET01, RET03, RET07 and RET14 in the figure). Gene names are on the x-axis, and GO or Reactome terms on the y-axis. Fold changes compared to the control group are expressed as $\log_2$ values and the color scale indicates the intensity. The color scale is the same for all heat maps.

Fig. 6. Heat maps of the ORAs output for pyrene (32 µg.L^{-1}) and phenanthrene (100 µg.L^{-1}) after 1 or 14 days of exposure (shortened as PYR01, PYR14 and PHE14 in the figure). No significant over-represented GO terms were found after either 3 or 7 days of exposure. Gene names are on the x-axis and GO terms on the y-axis. Fold changes compared to the control group are expressed as $\log_2$ values and the color scale indicates the intensity. The color scale is the same for both heat maps.

Declaration of competing interests

☒ The authors declare that they have no known competing financial interests or personal relationships that could have appeared to influence the work reported in this paper.

☐The authors declare the following financial interests/personal relationships which may be considered as potential competing interests:

Author contributions

Cyril Rigaud: Conceptualization, Methodology, Data Acquisition, Data Analysis, Writing – Original Draft. **Andreas Eriksson:** Conceptualization, Methodology, Data Acquisition, Data Analysis, Writing – Review & Editing. **Aleksei Krasnov:** Methodology, Data Acquisition, Data Analysis. **Emma Wincent:** Methodology, Data Acquisition, Writing – Review & Editing. **Hannu Pakkanen:** Methodology. **Heli Lehtivuori:** Methodology. **Janne Ihalainen:** Methodology. **Eeva-Riikka Vehniäinen:** Conceptualization, Methodology, Funding Acquisition, Project Administration, Supervision, Writing – Review & Editing.

Graphical abstract

Highlights

- Rainbow trout larvae were exposed to either retene, pyrene or phenanthrene.
- Their effects on the cardiac transcriptome were assessed using custom microarrays.
- Very few differentially expressed genes were shared between PAHs.
- Retene was the most potent compound and altered key cardiac genes.
- Retene and pyrene both altered myosin-related genes, but in an opposite direction.

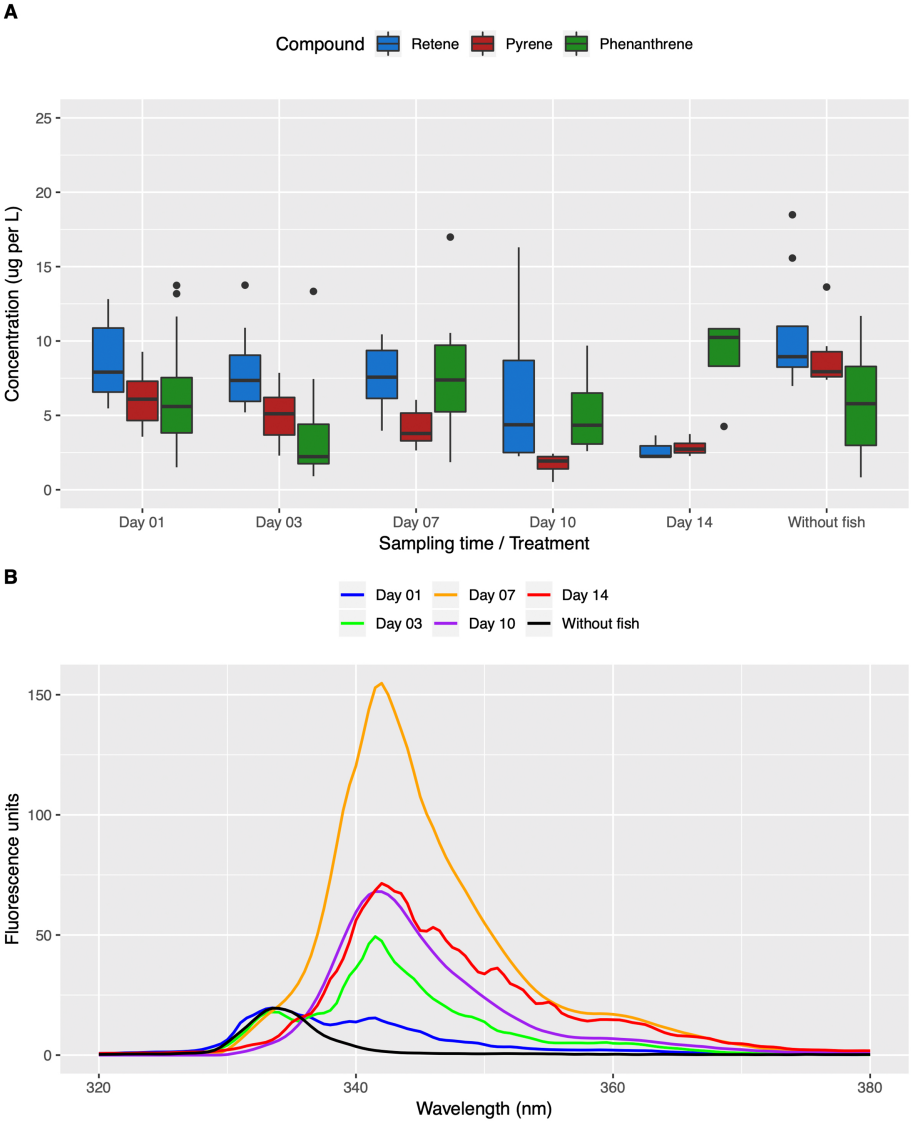
A
Compound
Retene
Pyrene
Phenanthrene
Concentration (ug per L)
25
20
15
10
5
0
Day 01
Day 03
Day 07
Day 10
Day 14
Without fish
Sampling time / Treatment
B
Day 01
Day 03
Day 07
Day 10
Day 14
Without fish
Fluorescence units
150
100
50
0
320
340
360
380
Wavelength (nm)

Figure 1

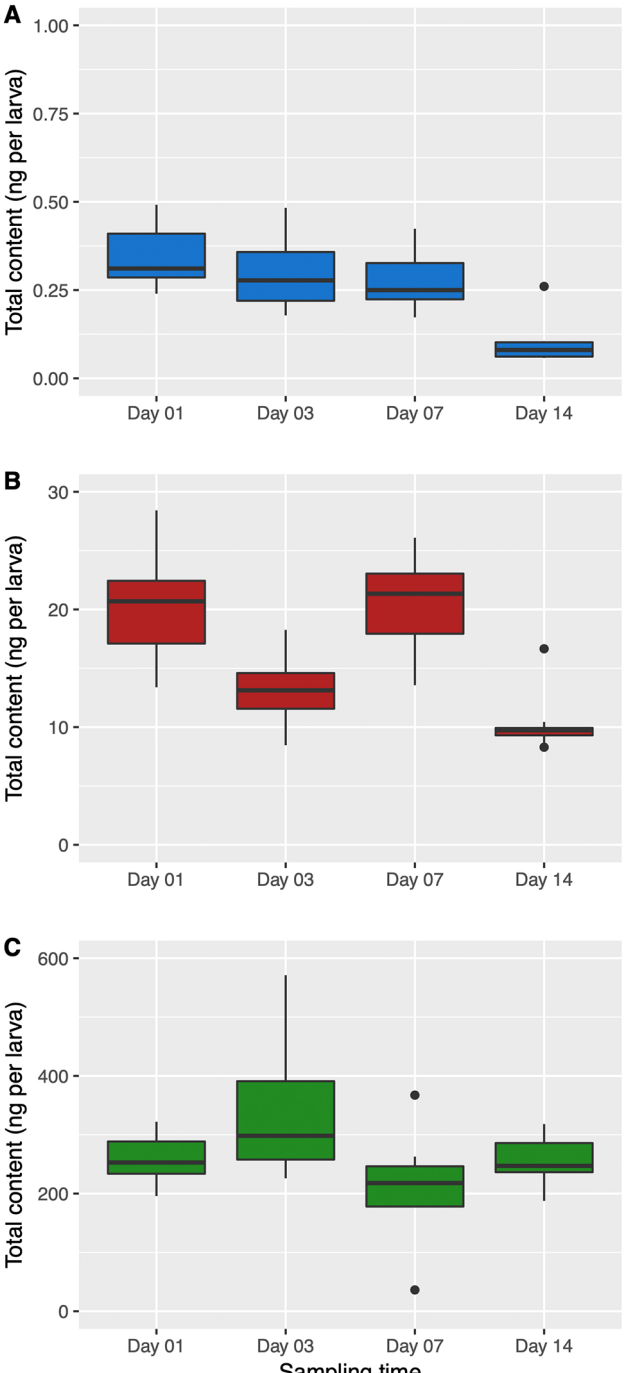
A
Total content (ng per larva)
1.00
0.75
0.50
0.25
0.00
Day 01
Day 03
Day 07
Day 14
B
Total content (ng per larva)
30
20
10
0
Day 01
Day 03
Day 07
Day 14
C
Total content (ng per larva)
600
400
200
0
Day 01
Day 03
Day 07
Day 14
Sampling time

Figure 2

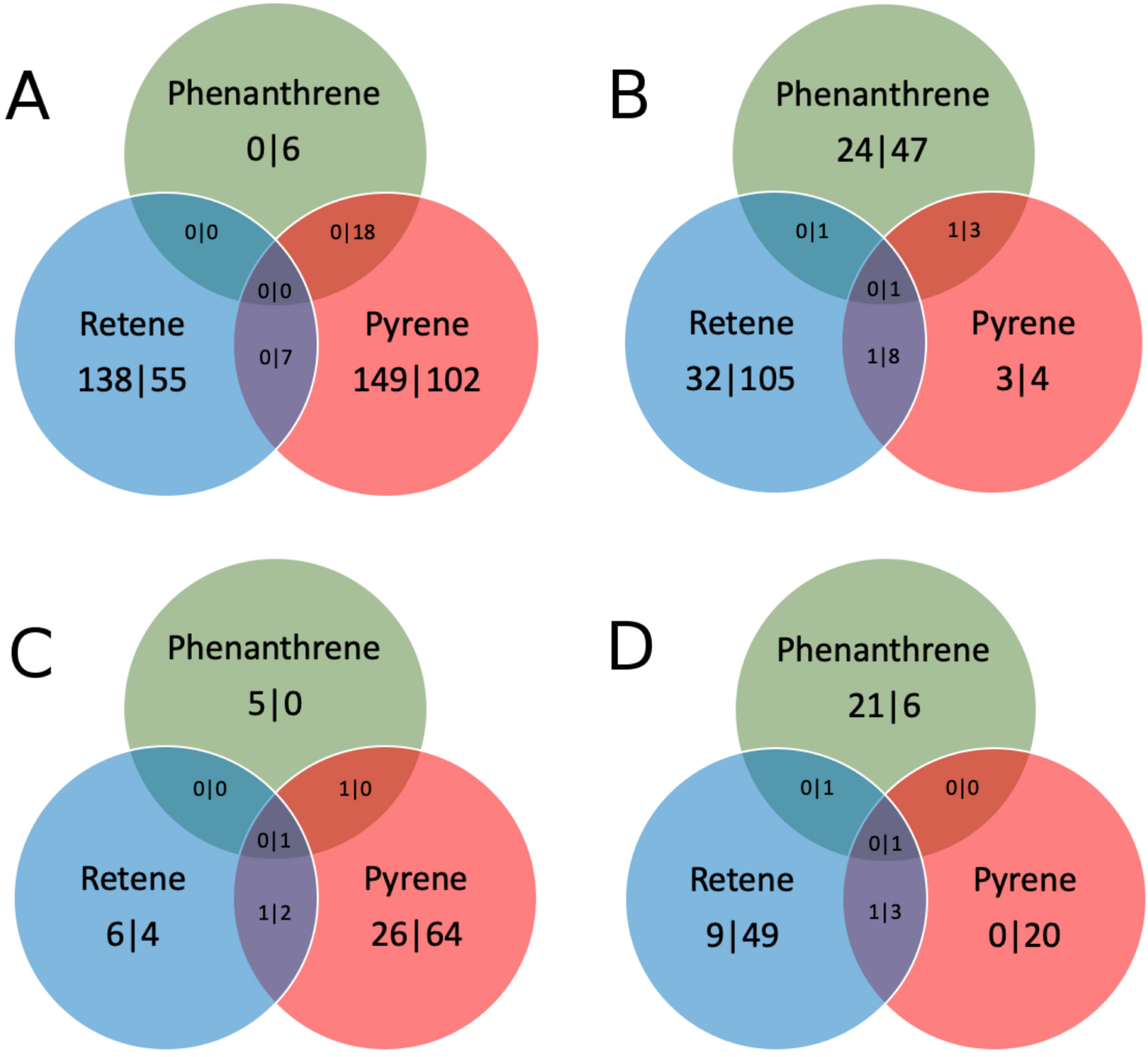
A
Phenanthrene
0|6
0|0
0|18
0|0
Retene
138|55
0|7
Pyrene
149|102
B
Phenanthrene
24|47
0|1
1|3
0|1
Retene
32|105
1|8
Pyrene
3|4
C
Phenanthrene
5|0
0|0
1|0
0|1
Retene
6|4
1|2
Pyrene
26|64
D
Phenanthrene
21|6
0|1
0|0
0|1
Retene
9|49
1|3
Pyrene
0|20

Figure 3

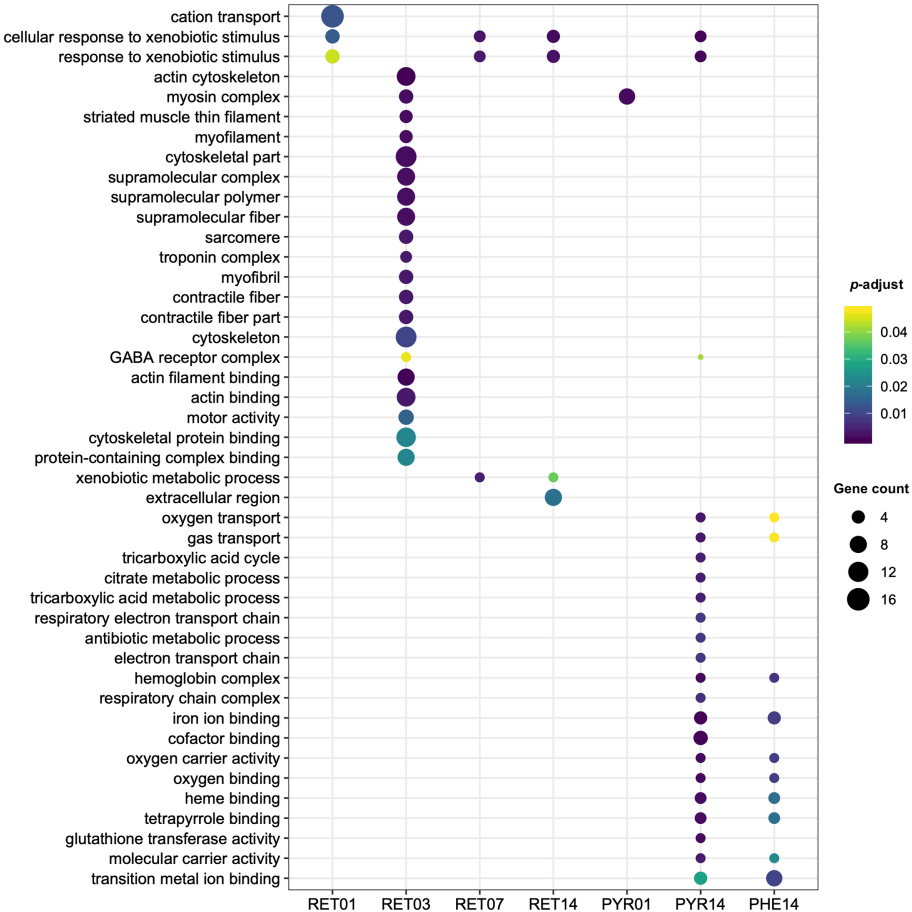
cation transport
cellular response to xenobiotic stimulus
response to xenobiotic stimulus
actin cytoskeleton
myosin complex
striated muscle thin filament
myofilament
cytoskeletal part
supramolecular complex
supramolecular polymer
supramolecular fiber
sarcomere
troponin complex
myofibril
contractile fiber
contractile fiber part
cytoskeleton
GABA receptor complex
actin filament binding
actin binding
motor activity
cytoskeletal protein binding
protein-containing complex binding
xenobiotic metabolic process
extracellular region
oxygen transport
gas transport
tricarboxylic acid cycle
citrate metabolic process
tricarboxylic acid metabolic process
respiratory electron transport chain
antibiotic metabolic process
electron transport chain
hemoglobin complex
respiratory chain complex
iron ion binding
cofactor binding
oxygen carrier activity
oxygen binding
heme binding
tetrapyrrole binding
glutathione transferase activity
molecular carrier activity
transition metal ion binding
RET01
RET03
RET07
RET14
PYR01
PYR14
PHE14
p-adjust
0.04
0.03
0.02
0.01
Gene count
4
8
12
16

Figure 4

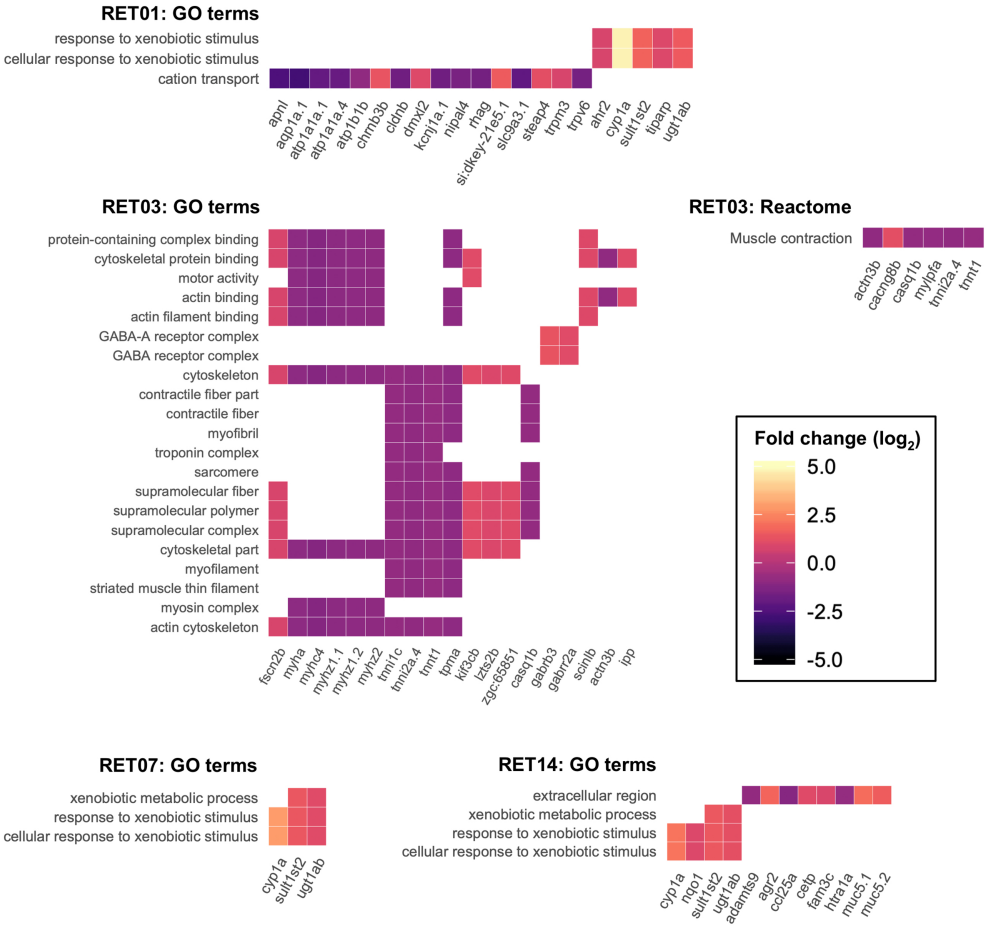
RET01: GO terms
response to xenobiotic stimulus
cellular response to xenobiotic stimulus
cation transport
apnl
aqp1a.1
atp1a1a.1
atp1a1a.4
atp1b1b
chmb3b
cldnb
dmxl2
kcnj1a.1
nipal4
rhag
si:dkey-21e5.1
slc9a3.1
steap4
trpm3
trpv6
ahr2
cyp1a
sult1st2
tiparp
ugt1ab
RET03: GO terms
protein-containing complex binding
cytoskeletal protein binding
motor activity
actin binding
actin filament binding
GABA-A receptor complex
GABA receptor complex
cytoskeleton
contractile fiber part
contractile fiber
myofibril
troponin complex
sarcomere
supramolecular fiber
supramolecular polymer
supramolecular complex
cytoskeletal part
myofilament
striated muscle thin filament
myosin complex
actin cytoskeleton
fscn2b
myha
myhc4
myhz1.1
myhz1.2
myhz2
tnni1c
tnni2a.4
tnnt1
tpma
kif5cb
lzts2b
zgc:65851
casq1b
gabrb3
gabrr2a
scinlb
actn3b
ipp
RET03: Reactome
Muscle contraction
actn3b
cacng6b
casq1b
mylpfa
tnni2a.4
tnnt1
Fold change (log2)
5.0
2.5
0.0
-2.5
-5.0
RET07: GO terms
xenobiotic metabolic process
response to xenobiotic stimulus
cellular response to xenobiotic stimulus
cyp1a
sult1st2
ugt1ab
RET14: GO terms
extracellular region
xenobiotic metabolic process
response to xenobiotic stimulus
cellular response to xenobiotic stimulus
cyp1a
nqo1
sult1st2
ugt1ab
adamts9
agr2
ccl25a
celp
fam3c
htra1a
muc5.1
muc5.2

Figure 5

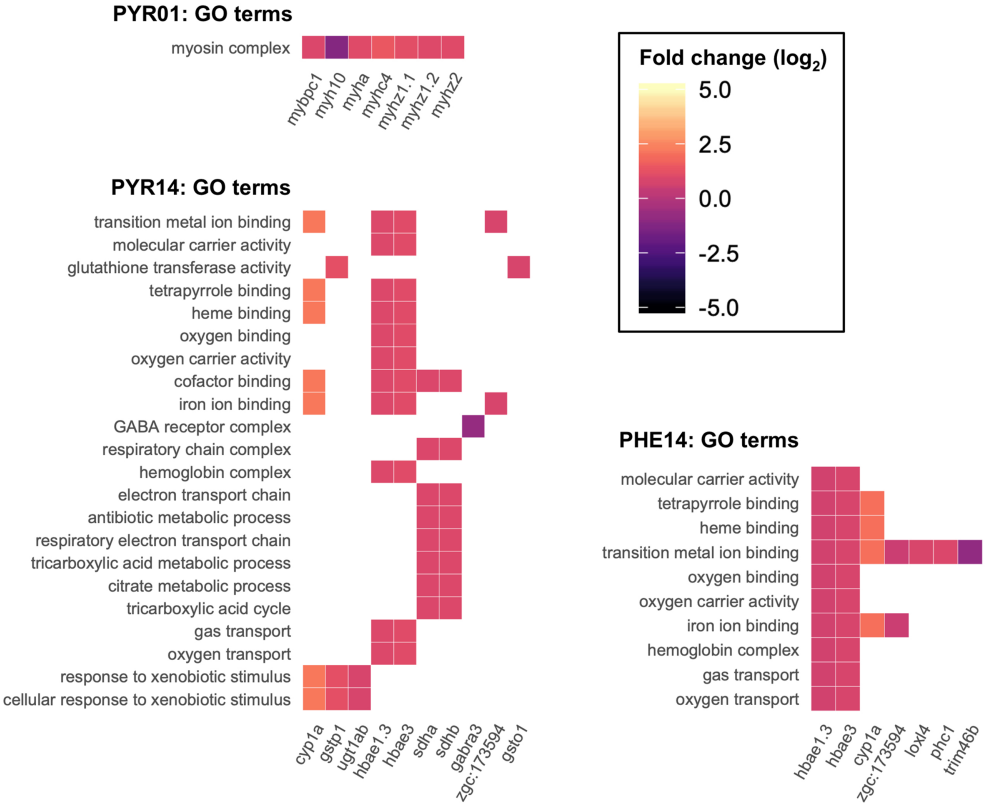
PYR01: GO terms
myosin complex
mybpc1
myh10
myha
myhc4
myhz1.1
myhz1.2
myhz2
Fold change (log2)
5.0
2.5
0.0
-2.5
-5.0
PYR14: GO terms
transition metal ion binding
molecular carrier activity
glutathione transferase activity
tetrapyrrole binding
heme binding
oxygen binding
oxygen carrier activity
cofactor binding
iron ion binding
GABA receptor complex
respiratory chain complex
hemoglobin complex
electron transport chain
antibiotic metabolic process
respiratory electron transport chain
tricarboxylic acid metabolic process
citrate metabolic process
tricarboxylic acid cycle
gas transport
oxygen transport
response to xenobiotic stimulus
cellular response to xenobiotic stimulus
cyp1a
gstp1
ugt1ab
hbae1.3
hbae3
sdha
sdhb
gabra3
zgc:173594
gsto1
PHE14: GO terms
molecular carrier activity
tetrapyrrole binding
heme binding
transition metal ion binding
oxygen binding
oxygen carrier activity
iron ion binding
hemoglobin complex
gas transport
oxygen transport
hbae1.3
hbae3
cyp1a
zgc:173594
loxl4
phc1
trim46b

Figure 6